UNSYS digital

International Journal of Robotics and Mechatronics

Ducted Fan Flying Object with Normal and Reverse Ducted Fan Units

Masafumi Miwa[†] and Shinya Marubashi[§]

[†]Institute of Technology & Science, The University of Tokushima, Japan

[§]The University of Tokushima, Japan

***Abstract*—**Recently, UAV such as single or multi rotor helicopter is used in aerial photography and aerial investigation. However, rotor blades of UAV's thrust device are not covered by propeller guard, and the thrust is generated by high rotational speed. Thus UAV has a high risk of damage. In previous study, we presented inverted pendulum type flying object (DFO1 and DFO2) using ducted fans instead of rotor blades. PI-D control was employed for roll, pitch and yaw attitude control. We succeeded to achieve stable hovering by 3-axes (roll, pitch and yaw axis) attitude control. However, small oscillations and small steady state errors appear. These oscillations and steady state errors can be attributed to Gyro moment of ducted fan tilting motion. In this study, we report a newly developed DFO3 equipped with normal and reverse rotation ducted fan to cancel Gyro moment effect. We succeeded to achieve stable takeoff/landing and hovering.

***Keywords*—**UAV, ducted fan, attitude control, inverted pendulum.

I. Introduction

In recent years, light aircrafts and helicopters are used in fields of aerial photography and aerial investigations. However, UAV (unmanned aerial vehicle) such as radio controlled (R/C) helicopter takes the place of the real aircraft in proportion to the improvement of the radio control technology. The operation cost of the R/C helicopter is lower than the actual one. In addition, required heliport size is smaller than that of actual one. Thus, the R/C helicopter has reasons why those are more excellent than an actual one, there are many reports of automatic control system for R/C helicopter [1][2][3], and some additional auto pilot units are available in the market. Also another type of autonomous UAV such as quad rotor helicopter [4] (more stable), tilt rotor plane [5] (long cruising distance), tail-sitter [6] (fixed wing VTOL) were reported.

However, UAV operation still involves risks, and it causes fatal accidents and serious injury. An inexperienced operator, radio wave interference, wind disturbance, etc., are the factors responsible for these accidents. These UAV obtain thrust generated by rotor blades with very high rotating speed, and it makes UAV as dangerous device. Additionally, Thrusters of these UAV are set on upper or front level of Center Of Gravity (COG). This structure has an advantage that gravity acts on the airframe as horizontal stabilizer. On the other hand, it is difficult to hang payload to the airframe directly because thruster backwash exists.

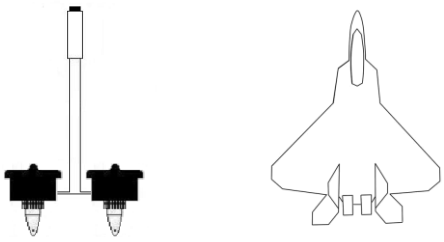

(a) Ducted fan flying object **(b) Pusher type aircraft**

Figure 1 Model of ducted fan flying object and inverted aircraft [7]

To clear up the risk of rotor blade and thruster backwash influence for payload, we presented new flying machines that use ducted fans instead of rotor blades [7][8]. **Figure 1(a)** shows inverted pendulum type airframe named as "DFO" [7]. Size of the ducted fan is small and rotor wing is placed inside the duct. So ducted fan help to decrease accident risk. We present the DFO as a pusher type inverted VTOL UAV similar to an inverted pendulum, because the inverted airframe has an advantage to cut down the takeoff/landing area. The dynamic model of DFO is same as a pusher type aircraft when it flies vertically as shown in **Figure 1(b)**. It is clear that DFO has COG above thruster units which cause instability on attitude of DFO airframe by gravity and it is the disadvantage of inverted airframe. In our previous study, attitude control method by thrust vectoring with servomotors was reported [7]. Also, hovering maneuver is controlled by three axes thrust vectoring (roll axis, pitch axis, and yaw axis) using servomotors. We succeeded to achieve stable hovering by 3-axes (roll, pitch and yaw axis) attitude control. However, small oscillation and small steady state error appears. These oscillation and steady state error can be attributed to Gyro moment of ducted fan tilting motion. In this study, we report a newly developed DFO3 (DFO ver.3) equipped with normal and reverse rotation ducted fan to cancel Gyro moment effect. We succeeded to achieve stable take off / landing and hovering.

Corresponding author: Masafumi Miwa (e-mail: miw@tokushima-u.ac.jp).
This paper was submitted on February 15, 2014; revised on April 09, 2014; and accepted on May 14, 2014.

II. Ducted Fan Flying Object [7]

Figure 2, 3 and **4** show the axes of DFO. Each axis is rotated with the torque expressed by multiplication of thrust component and distance from COG to ducted fan. Thrust component is generated by titling the ducted fan with servo motor. In this study, we assume that each rotational motion on 3-axes (roll, pitch, and yaw) is controllable independently when the attitude angles are small.

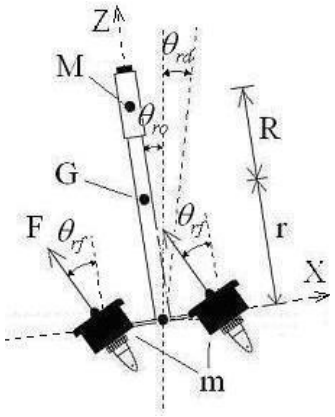

Figure 2 Rotation model of roll axis

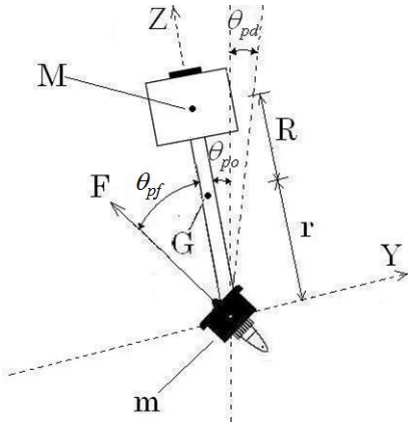

Figure 3 Rotation model of pitch axis

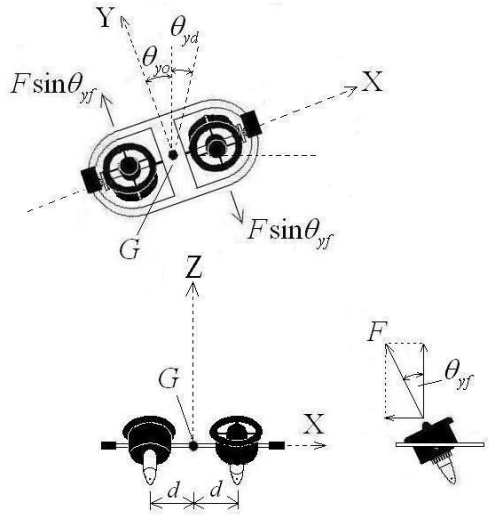

Figure 4 Rotation model of yaw axis

Figure 2 shows the roll axis rotational motion model of DFO, where θ_{rd} is the target attitude angle of DFO, θ_{rf} is angle of the ducted fan tilted by the servo motor. θ_{ro} is attitude angle of DFO, G is the center of gravity, M is the mass of airframe (includes battery, sensors and CPU, etc.), m is the mass of the ducted fan units, R is the distance between to G and M, r is the distance between G and m. And J_r, J_p, and J_y are entire moment of inertia of the airframe on roll, pitch and yaw axis, respectively.

The equation of motion becomes Equation (1).

$$J_r\ddot{\theta}_{ro} = rF\sin\theta_{rf} - MgR\sin\theta_{ro} + mgr\sin\theta_{ro} \quad (1)$$

From the centrobaric momentum equilibrium, $MgR\sin\theta_{ro}$ and $mgr\sin\theta_{ro}$ are countering with each other. When θ is so small, $\sin\theta \cong \theta$. Using Laplace transform, Eq. (1) is converted to Eq. (2) as below.

$$s^2\Theta_{ro}J_r = rF\Theta_{rf} \quad (2)$$

From Equation (2), transfer function of DFO's attitude of roll axis is expressed in Eq. (3).

$$\frac{\Theta_{ro}}{\Theta_{rf}} = \frac{rF}{J_r s^2} \quad (3)$$

Figure 3 shows the pitch axis rotational motion model of DFO, where θ_{pd} is the target attitude angle of DFO, θ_{pf} is angle of the ducted fan tilted by the servo motor. θ_{po} is attitude angle of DFO. According to the calculation in the same way, transfer function of DFO's attitude of pitch axis is expressed in Eq. (4).

$$\frac{\Theta_{po}}{\Theta_{pf}} = \frac{rF}{J_p s^2} \quad (4)$$

Figure 5 shows the yaw axis rotational motion model of DFO, where θ_{yd} is the target attitude angle of yaw axis, θ_{yo} is rotating angle of yaw axis, d is the distance between yaw axis and the center of ducted fan, F is thrust of ducted fan, and θ_{yf} is the tilted angle of ducted fan. The equation of yaw axis rotational motion is expressed in Equation (5),

$$J_y\ddot{\theta}_{yo} = 2dF\sin\theta_{yf} \quad (5)$$

When θ_{yf} is so small, Equation (5) is converted to Eq. (6) by Laplace transform.

$$s^2\Theta_{yo}J_y = 2dF\Theta_{yf} \quad (6)$$

From Equation (6), transfer function of DFO's yaw axis rotation is expressed in Equation (7).

$$\frac{\Theta_{yo}}{\Theta_{yf}} = \frac{2dF}{J_y s^2} \quad (7)$$

III. Experimental Methods and Results

A. Experimental setup

Figure 5 shows the schematic diagram of experimental

setup. ArduPilotMega2.0 (APM: 3DRobotics) is used as a flight controller for test airframe. APM includes IMU (Inertial Measurement Unit consists of one-chip 3 axes gyro/ acceleration sensor and one-chip 3axes magnetic sensor) and barometric altimeter. APM is linked with PC via XBee (XBee Pro ZB: Digi International). Radio controller set (transmitter 12FG and receiver R149DP: Futaba) is used for experiments operation. We can control DFO3 by sending target angles of 3 axes and throttle with this radio controller set. Flight test program on APM is constructed from library programs of Arducopter 3.0.1 (freeware: DIY Drones [9]). APM receives triaxial angle and angular velocity from IMU. APM transmits PWM signal for two ducted fan drive amplifiers (Multistar Opto 45A: TURNIGY) and 4 servo motors (S3005: Futaba) to control thrust and its direction. **Figure 6** shows the experimental setup of DFO3. Airframe of DFO3 is made of plywood plate (4 mm thickness) cut by laser cutter.

DFO3 consists of positive rotation ducted fan and reverse rotation ducted fan (70 mm ducted fan: Free Wing). Each ducted fan is mounted on gimbals respectively. Four servomotors are capable of tilting these ducted fans along roll and pitch axis, independently, which act as yaw (rudder), pitch (elevator) and roll (aileron) axis controller of airframe. Two lithium polymer batteries (14.8V-4S- 2200mAh: Kypom) are used for each ducted fan and controller. Maximum thrust of the experimental ducted fan is 1200 gf. Experimental airframe has two ducted fans; therefore, total thrust is 2400 gf while experimental airframe weight is 1560 g. Basic feature of DFO3 is similar to that of DFO2 except ducted fan and radio control system.

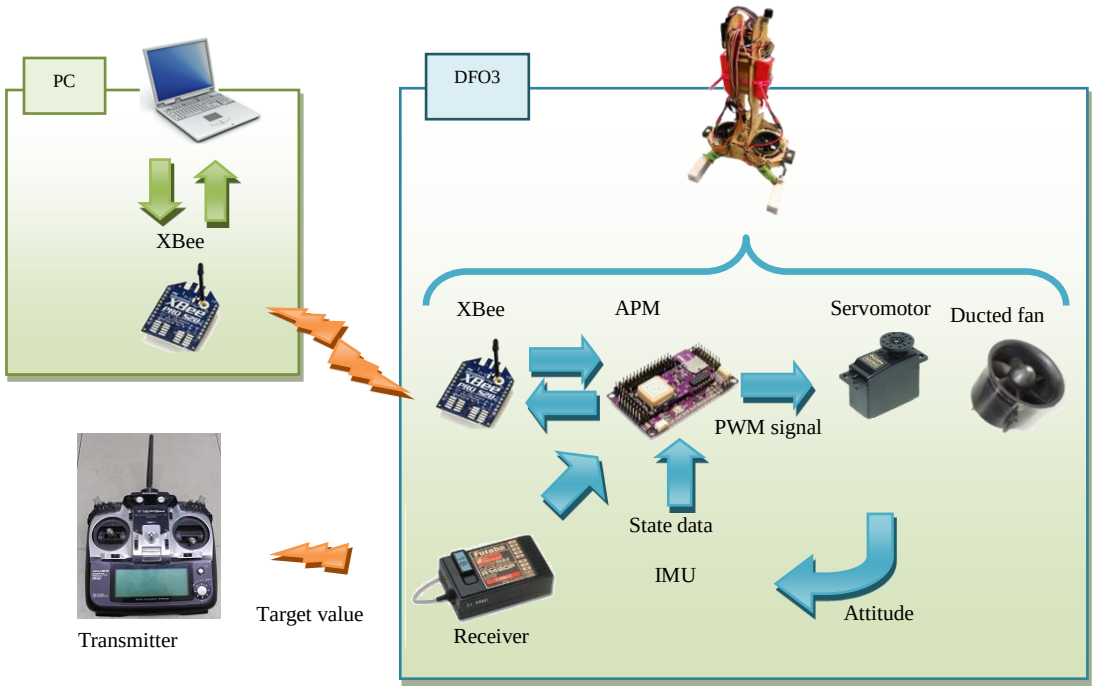

Figure 5 Schematic diagram of experimental setup

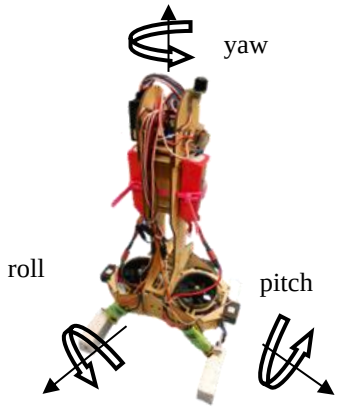

Height	520mm
Width	295mm
Weight	1560g
Thrust	2400gf
Duct Diameter	70mm
Flight time	5min
J_r	39.36×10^{-3} kg m^2
J_p	35.42×10^{-3} kg m^2
J_y	9.17×10^{-3} kg m^2

Figure 6 Experimental airframe (DFO3)

B. Attitude control system

PI-D control was adopted for attitude control of roll, pitch and yaw axis, independently. **Figure 7** and **Figure 8** represents the block diagram of PI-D control system of roll / pitch and yaw axes, where, K_p is P gain, K_D is D gain, K_I is I gain, G_M is the transfer function of servomotor. G_M was measured experimentally, J (J_r or J_p), and J_y were estimated from CAD data. PI-D control systems of roll, pitch and yaw axes are same.

TABLE I shows PID parameters. PI-D control parameters were decided by pole assignment method and simulation results.

TABLE I PID Parameters

	P Gain	I Gain	D Gain
Roll axis	1.6774	0.0907	0.2271
Pitch axis	1.5095	0.0817	0.2043
Yaw axis	0.7237	0.0392	0.0980

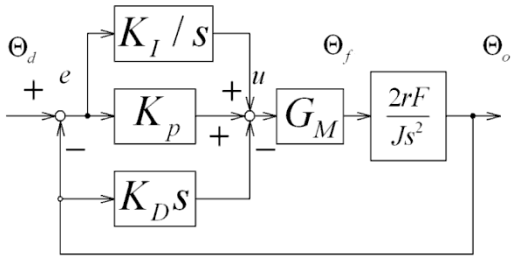

Figure 7 PI-D control system (roll/pitch axis) [7]

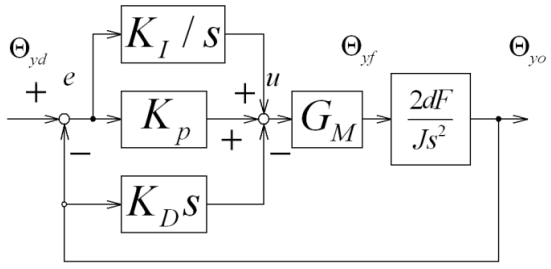

Figure 8 PI-D control system (yaw axis) [7]

C. Experiment 1: Hovering Test and Trim Setting

Hovering test was carried out with estimated gain parameters of **Table I**. Experiments were performed as follows.

Step 1: Test airframe was held by hands. (**Figure 9(a)**)
Step 2: Throttle was increased until thrust balances weight.
Step 3: Test airframe was released when thrust balanced to weight (**Figure 9(b)**).
Step 4: Test airframe was caught by hand, and experiment was completed.

Figure 9 shows scenes of hovering test, and **Figure 10** shows the result of hovering test with parameters estimated by simulation. In **Figure10**, test airframe was released at the 21st second. It started to fall, but throttle was increased immediately to keep the height by manual control. Hovering performance of test airframe was good, and it hovered stably. Unlike the previous study, we can control test frame by radio transmitter. Thus, it is easy to control attitude and altitude of test airframe. Test airframe landed at the 31st second by manual control.

Test airframe was drifted a little during hovering maneuver because position control was not installed yet. Therefore, we tuned the trim as target angle offsets of roll and pitch attitude control that reduce airframe drift by repeated experiments. These target angle offsets are not zero but vertical component of thrust passes the COG of test airframe when attitude converge to the target angle. We use "trim" function of radio transmitter to set these target angle offset. **Table II** shows target angle offsets.

(a) Before release

(b) After release

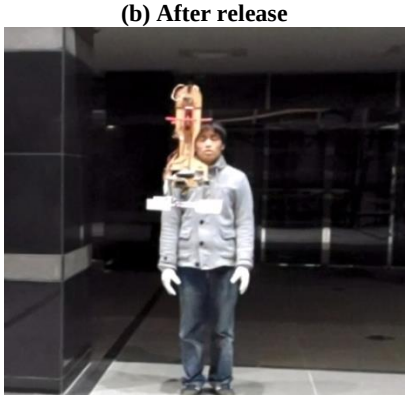

(c) Hovering

Figure 9 Scene of hovering test

TABLE II Target angle offsets

	Target angle offset (degree)
Roll axis	-0.56
Pitch axis	-2.96

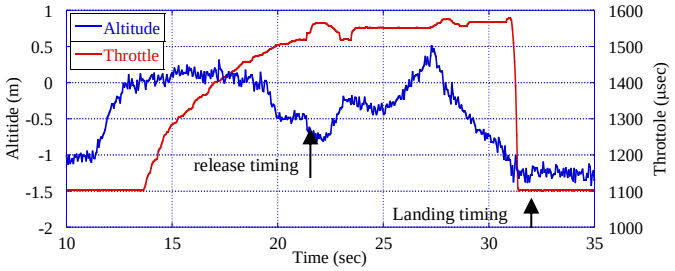

(a) Altitude

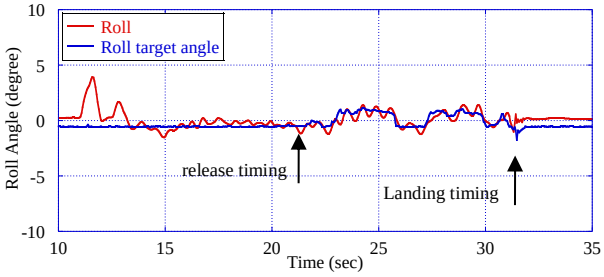

(b) Roll

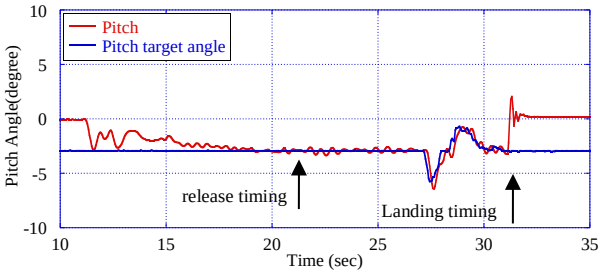

(c) Pitch

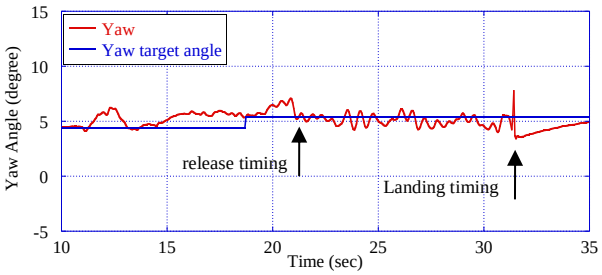

(d) Yaw

Figure 10 Results of hovering test

D. Experiment 2: Manual Flight Test

Next, we tried manual flight test. Target angles of attitude and throttle were operated by manual operation. Manual flight test was done as followings.

Step 1: Test airframe was set on floor, and offset target angles of each 3 axis were set.
Step 2: Each PI-D control was started.
Step 3: Throttle was opened slowly.
Step 4: After DFO3 took off and it reached appropriate height, throttle was controlled to hold the height.
Step 5: Target angles were sent from radio control transmitter.
Step 6: Throttle was closed slowly to land.

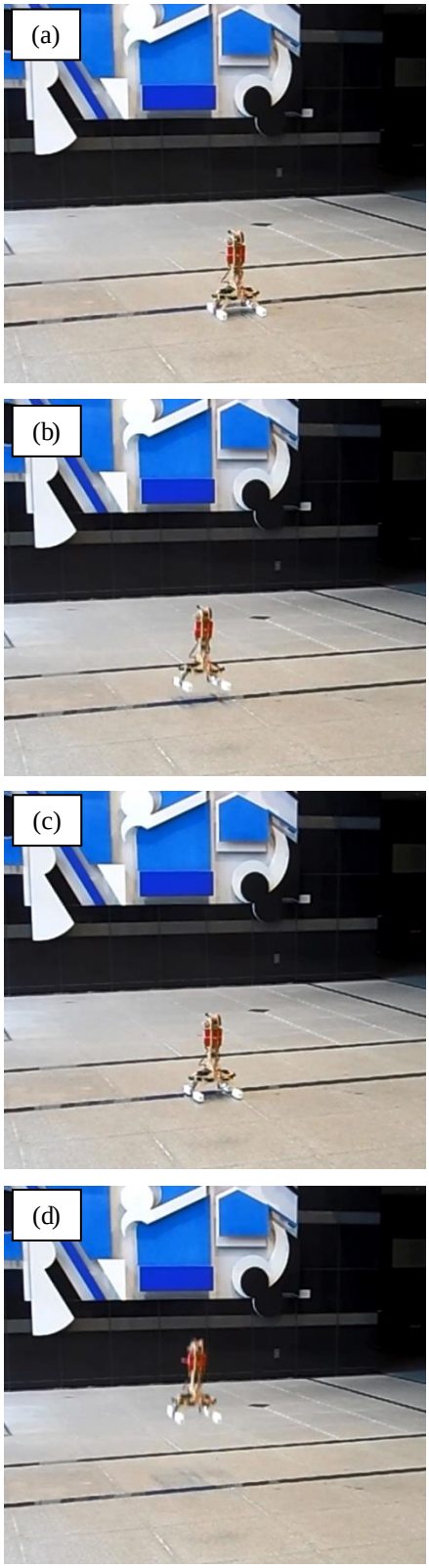

Figure 11 Test scene of take-off test

Figure 11 shows the scene of takeoff and **Figure 12** shows altitude and attitude during takeoff. At first, test airframe was set on the floor, and offset target angles of **Table II** were set. Then test operator increased throttle slowly (**Figure 11(a)**). With increasing of thrust, test airframe started to shift (at the 5th second in **Figure 12** and **Figure 11(b)**). Because target angle offsets are setting for stable hovering in air, they will generate horizontal component of thrust when test airframe is on ground. So operator added negative angle to roll and positive angle to pitch until test airframe took off (at the 6th second in **Figure 12** and **Figure 11(c)**). No operation was added to yaw axis because yaw was stable.

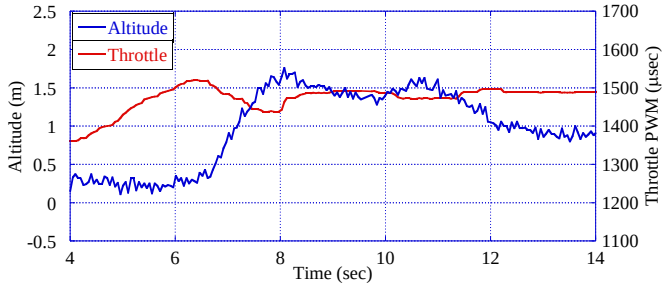

(a) Altitude

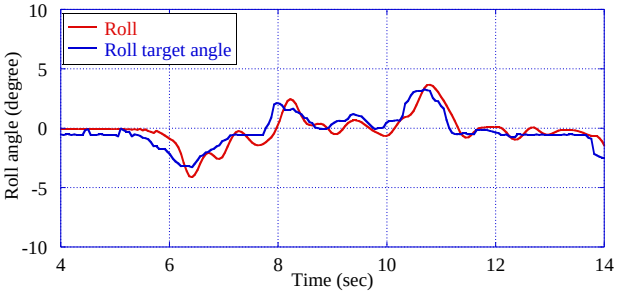

(b) Roll axis

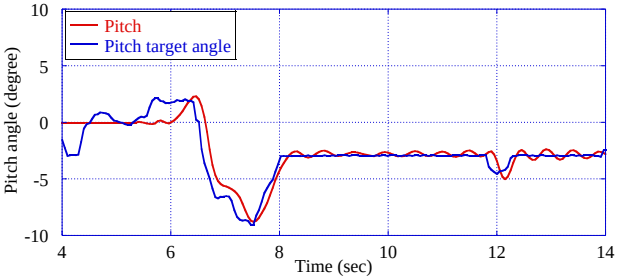

(c) Pitch axis

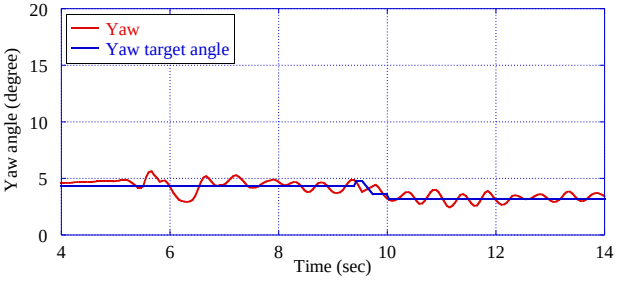

(d) Yaw axis

Figure 12 Response of PI-D control during take-off test

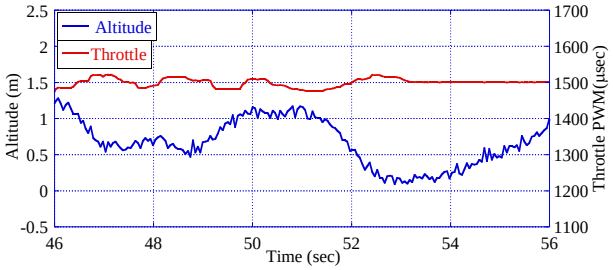

(a) Altitude

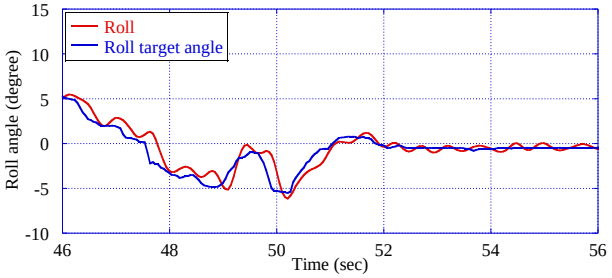

(b) Roll axis

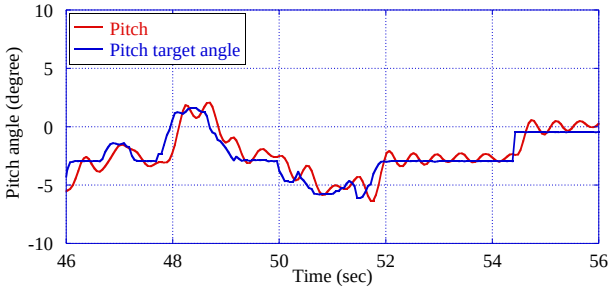

(c) Pitch axis

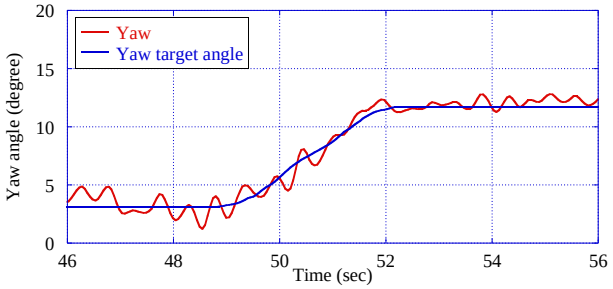

(d) Yaw axis

Figure 13 Response of PI-D control during manual flight

In previous study of DFO2, yaw angle rotated about 10 degrees before takeoff timing. This rotation was caused by counter torque of ducted fan and the frictional force change between DFO2 landing gear and floor. The friction force cancels the counter torque of ducted fans until takeoff timing, and PI-D control of yaw axis does not work because friction force hold yaw angle. Takeoff procedure decreases frictional force. With quick decrement of friction force with takeoff, the counter torque rotates DFO2. Then PI-D control will correct yaw angle to target angle. On the other hand, yaw rotation of DFO3 at takeoff timing is as small as 2 degrees since the counter torque is cancelled by reverse rotation of ducted fan. Additionally, this 2 degrees change was the rotation of test airframe subjected to the drift of the aircraft, and the center of

rotation was the last contact point of landing gear. Reverse rotation of ducted fan contributes to the stability of the yaw axis control.

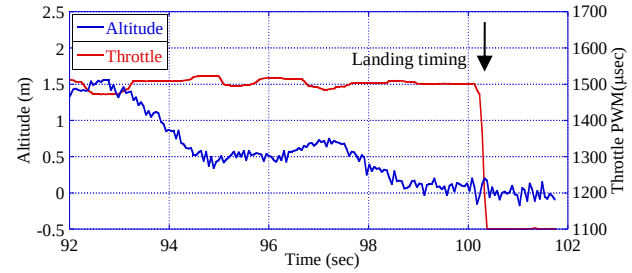

(a) Altitude

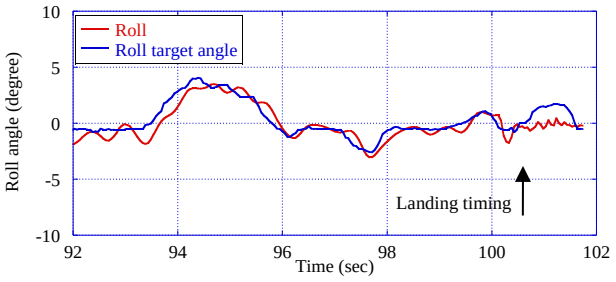

(b) Roll axis

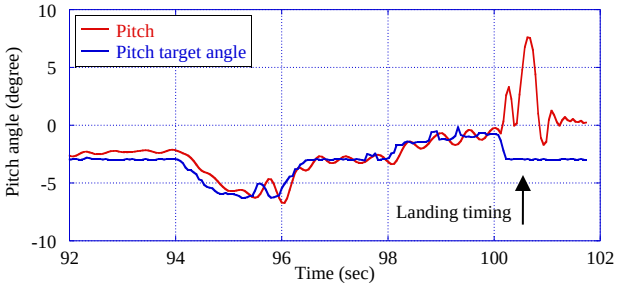

(c) Pitch axis

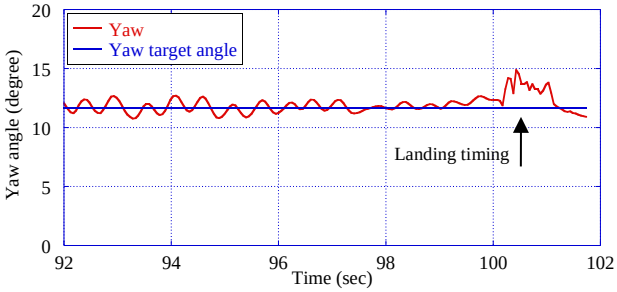

(d) Yaw axis

Figure 14 Response of PI-D control during landing

After takeoff when test airframe started to shift in the X axis direction, the operator retuned the target angles of pitch to neutral, and at the same time added correct rudder of roll to cancel the drift. When new target angle was set, PI-D control tilts the DFO airframe to the target angle. Then, ducted fan is tilted to hold the DFO attitude, and it generates thrust horizontal component. This component will move DFO. So we can be able to move DFO by tilting it. Also throttle was controlled to keep the height of test airframe. At the 9.5th second in **Figure 12**, yaw target angle was changed, and test airframe followed the new target angle well.

Figure 13 shows altitude and attitude during manual flight and **Figure 15** shows the scenes of manual flight. Attitude angles followed the trend similar to target angles, DFO3 moved following to desired direction with small vibration. Vibration centers were followed by each target angle and the amplitude was about 1 degree. These vibrations will be suppressed by adjusting the PI-D parameters.

Figure 14 shows altitude and attitude during landing. Before landing operation, operator lowered the altitude of test airframe by tuning throttle precisely until the 95th second as shown in **Figure 14(a)**. Then operator controlled the test airframe to move to landing point until the 97th second as in **Figure 14**. In this period, target offset values were effective, so test airframe position was stable but attitude did not keep level. Thus, operator used radio controller to adjust the attitude to keep level during landing operation, and tuned throttle from the 97th to 100th second as shown in **Figure 14(a)**. At the 100th second, test airframe touched the floor with some vibrations accordingly, and then operator closed throttle to complete landing procedure.

Figure 16 and **Figure 17** show short flight result with step input of DFO3 and DFO2, respectively. Vibration amplitude of DFO3 is about 1 degree, and it seems to be attenuated slowly. On the other hand, vibration amplitude of DFO2 seems to diverge gradually. The main difference between DFO3 and DFO2 is equipment of reverse rotation ducted fan. Ducted fan is a high rotational speed machine, and it will generate gyro moment when it tilted in a large angle.

Figure 15 Scenes of manual flight

Target angle was changed in manual flight as shown in **Figure 16** and in **Figure 17**, ducted fan was tilted in a large angle, thus it generated large gyro moment. In DFO2 case, both ducted fan generated same direction of gyro moment and this doubled the gyro moment effects on attitude control. In contrast, gyro moments of normal rotation and reverse rotation ducted fan mounted on DFO3 cancel each other. Therefore, reaction of gyro moment of DFO3 on attitude control is small.

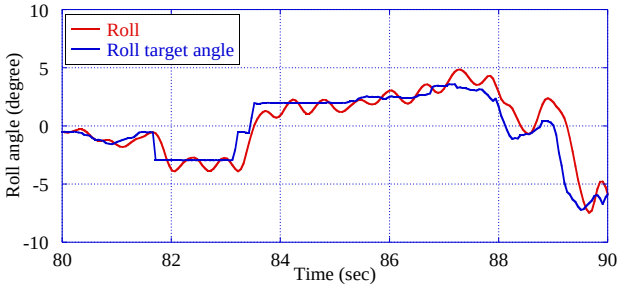

(a) Roll axis

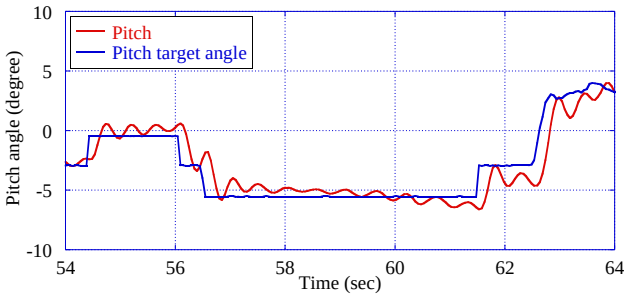

(b) Pitch axis

Figure 16 Attitude response of DFO3

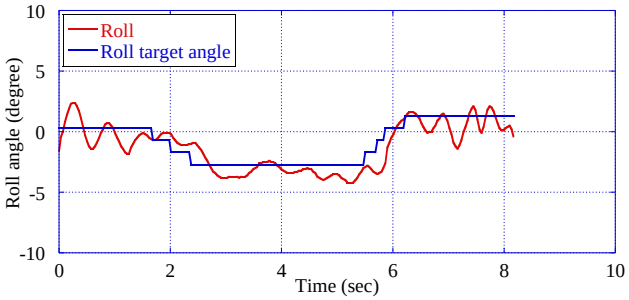

(a) Roll axis

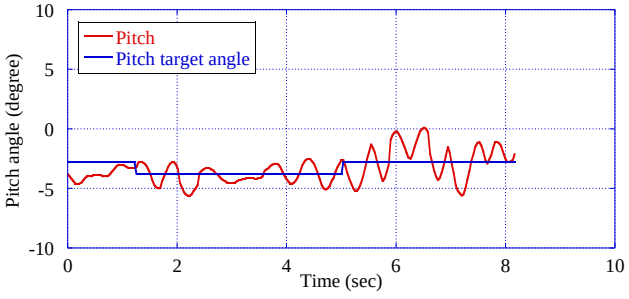

(b) Pitch axis

Figure 17 Attitude response of DFO2 [7]

IV. Conclusions

In this study, we developed DFO3 with reverse rotation ducted fan and radio control system. Reverse rotation ducted fan was introduced to cancel the gyro moment produced by high speed rotation of ducted fan. Radio control system was introduced to simplify the operation of test airframe experiment.

As the result of experiments, installation of reverse rotation ducted fan succeeded to decrease the amplitude of vibration at vicinity of target angle and the rotation around yaw axis at takeoff timing. Further, radio controller was simplified to operate attitude and altitude of test airframe. It became easy to execute takeoff operation and manual flight operation. However, small vibrations still remain. These vibrations can be suppressed by adjusting the PID parameters.

Flying time of DFO is shorter than normal aircraft because the maneuver of DFO is achieved by the reaction of ducted fan thrust only and it causes early battery drain. Moreover, the dynamic model of DFO is almost the same as a pusher type fixed wing aircraft when it flies vertically. So, we will develop a new DFO4 by applying this study results to a pusher type aircraft which equips thrust-vectoring. Takeoff/landing and hovering motion of DFO4 will be done with vertical mode (same as DFO1, 2 and 3) and DFO4 cruises in horizontal mode same as normal airplane. We will study DFO4 as a new type VTOL aircrafts in the near future.

References

[1] J. Shin, D. Fujiwara, K. Hazawa and K. Nonami, “Model Based Optimal Attitude and Positioning Control of Small-Scale Unmanned Helicopter”, Tran. Of the Japan Society of Mechanical Engineers, Vol.70, No.697 (2004), C, pp.2631-2637

[2] S. Suzuki, D. Nakazwa, K. Nonami and M. Tawara, “Attitude Control of Small Electric Helicopter by Using Quaternion Feedback”, Journal of System Design and Dynamics, Vol.5, No.2 (2011), pp.231-247. CrossRef

[3] M. Miwa, I. Shiraishi, M. Matsushima and K. Minami, “Remote Control Support System for R/C Helicopter, ServiceRobotics and Mechatronics”, (2010), pp.125-130, Springer-Verlag

[4] D. Pebrianti, F. Kendoul, S. Azrad, W. Wang and K. Nonami, “Autonomous Hovering and Landing of a Quad-rotor Micro Aerial Vehicle by Means of on Ground Stereo Vision System, Journal of System Design and Dynamics, Vol.4, No.2 (2010), pp.269-284. CrossRef

[5] S. Suzuki, R. Zhijia, Y. Horita, K. Nonami, G. Kimura, T. Bando, D. Hirabayashi, M. Furuya and K. Yasuda, “Attitude Control of Quad Rotors QTW-UAV with Tilt Wing Mechanism”, Journal of System Design and Dynamics, Vol.4, No.3 (2010), pp.416-428. CrossRef

[6] D. Kubo and S. Suzuki, “Transitional Flights of a Tail-Sitter Vertical Takeoff and Landing Small Aerial Robot”, Proceedings of 45th AIRCRAFT SYMPOSIUM, (2007) , Page2H2

[7] M. Miwa, Y. Shigematsu and T. Yamashita, “Control of Ducted Fan Flying Object Using Thrust Vectoring”, Journal of System Design and Dynamics, Vol.6, No.3, pp.322-334, 2012. CrossRef

[8] M. Miwa, S. Uemura, Y. Ishihara, A. Imamura, J. Shim and K. Ioi, “Evaluation of quad ducted-fan helicopter”, International Journal of Intelligent Unmanned Systems, 1-2 (2013), pp.187–198. CrossRef

[9] DIY Drones, http://diydrones.com/